Journal of Quantitative Spectroscopy & Radiative Transfer ▮ (▮▮▮▮) ▮▮▮–▮▮▮

Contents lists available at ScienceDirect

Journal of Quantitative Spectroscopy & Radiative Transfer

journal homepage: www.elsevier.com/locate/jqsrt

# Validation of $HNO_3$ spectroscopic parameters using atmospheric absorption and emission measurements

H. Tran [a,*], G. Brizzi [b], L. Gomez [a], A. Perrin [a], F. Hase [c], M. Ridolfi [d], J.-M. Hartmann [a]

[a] Laboratoire Interuniversitaire des Systèmes Atmosphériques (LISA), CNRS UMR 7583, Université de Paris Est, 61 Avenue du Général de Gaulle, 94010 Créteil Cedex, France

[b] Harvard-Smithsonian Center for Astrophysics, Atomic and Molecular Physics Division, Cambridge, MA 02138, USA

[c] Forschungszentrum Karlsruhe, Institute of Meteorology and Climate Research (IMK), P.O. Box 3640, D-76021 Karlsruhe, Germany

[d] Dipartimento di Chimica Fisica e Inorganica, Università di Bologna, Viale del Risorgimento 4, 40136 Bologna, Italy

ARTICLE INFO

*Article history:*
Received 3 July 2008
Received in revised form
24 September 2008
Accepted 25 September 2008

*Keywords:*
Nitric acid ($HNO_3$)
Line parameters
Atmospheric emission
Atmospheric absorption
Ground based solar absorption
SAO
MIPAS

ABSTRACT

The improved database of $HNO_3$ spectroscopic parameters in the 600–950 $cm^{-1}$ spectral region presented in [Gomez L, Tran H, Perrin A, Gamache RR, Laraia A, Orphal J, et al. Some improvements of the $HNO_3$ spectroscopic parameters in the spectral region from 600 to 950 $cm^{-1}$. JQSRT 2008, in press] is tested by comparisons between calculations and atmospheric remotely sensed absorption and emission spectra. The line parameters in the 11.3 μm region are validated using ground-based Fourier transform solar absorption measurements, whereas those in the 13.1 μm region are successfully tested using balloon-borne atmospheric emission spectra. In both regions, the quality of the line parameters and the consistency between band intensities is confirmed through comparisons with emission spectra collected by the satellite-borne MIPAS instrument.





## 1. Introduction

Nitric acid plays an important role in atmospheric chemistry since it acts as a reservoir of $NO_x$, which are directly involved in ozone destruction [1]. Infrared remote sensing techniques are routinely used to determine volume mixing ratio (vmr) profiles of $HNO_3$ in the atmosphere. For such retrievals, the 11.3 μm region is one of the most widely used, for spectra recorded by ground-based [2–4], balloon-borne [5–7] and space-borne spectrometers [8–17]. This spectral region is of particular interest since it contains the strong $\nu_5$ and $2\nu_9$ bands and, being centered in an atmospheric window, it is practically free of interfering contributions by other species. Due to their importance for remote sensing, $HNO_3$ spectra near 11.3 μm have been the subject of numerous laboratory spectroscopic studies (see [18] and references therein).

In our preceding paper [18], some of the $HNO_3$ spectroscopic parameters in the 600–950 $cm^{-1}$ spectral range have been improved with respect to the very recently updated edition of the HITRAN database [19]. Firstly, line parameters were added for the $\nu_5+\nu_6-\nu_6$ and $\nu_5+\nu_7-\nu_7$ hot bands, centered at 869.1 and 875.7 $cm^{-1}$, respectively. The second improvement concerns the air broadening coefficients and their temperature dependence for which semi-classical calculations were performed [20]. These transition dependent data then replaced the former values which were obtained [21] from an approximate extrapolation of a few existing measurements. Finally, a model was proposed in order to account for line-

* Corresponding author. Tel.: +33 145 176557; fax: +33 145 171564.
*E-mail address:* hatran@lisa.univ-paris12.fr (H. Tran).

0022-4073/$ - see front matter © 2008 Published by Elsevier Ltd.
doi:10.1016/j.jqsrt.2008.09.012

mixing effects within the Q branch of the $\nu_5+\nu_9-\nu_9$ hot band at 885.4 $cm^{-1}$. In addition to these modifications, the line intensities of the $\nu_6$ and $\nu_8$ bands (centered at 646.8 and 763.1 $cm^{-1}$, respectively) were improved. All these modifications, which were tested and validated using laboratory measurements, are described in detail in Ref. [18].

The present paper extends the test of the improved database by making comparisons between calculations and atmospheric absorption and emission spectra measured by various instruments. The changes performed in the 11.3 μm region are validated using ground-based Fourier transform solar absorption measurements, whereas those near 13.1 μm are successfully tested using balloon-borne atmospheric emission spectra. Finally, the quality of the new database and the consistency between band intensities in both regions are confirmed through comparisons with emission spectra collected by the satellite-borne MIPAS instrument.

## 2. Atmospheric spectra

Ground based solar absorption measurements were made in Kiruna (Sweden), early 2003, by the IMK group, using the high resolution Fourier transform spectrometer (0.003 $cm^{-1}$ resolution unapodized) described in Ref. [22]. Four of the spectra have been used in the present study, obtained for apparent solar elevation angles of 2.75°, 4.90°, 14.50° and 26.65°, respectively. They are calibrated to absolute radiance units and the atmospheric transmission for each recording is thus obtained by dividing the measured radiances by the extra-terrestrial solar value.

In the Smithsonian Astrophysical Observatory (SAO) experiment [23] a balloon-borne Fourier transform instrument (0.004 $cm^{-1}$ resolution unapodized) is used. The limb viewing emission data analyzed thereafter were obtained on 30 April 1997 over Alaska. They consist of nine radiance spectra in the 325–917 $cm^{-1}$ spectral range recorded at float (balloon at 40 km) for tangent heights from about 37 down to 10 km.

The Michelson interferometer for passive atmospheric sounding (MIPAS) experiment [24] is a spectrometer (0.0035 $cm^{-1}$ resolution unapodized) onboard the ENVISAT satellite. The MIPAS limb emission radiances used in this work are the same as those used in Ref. [17]. They were selected among the observations acquired during the "well-characterized" ENVISAT orbits 2081 and 2082 (July 2002), with nominal tangent altitudes of 12 and 24 km.

The species which provide the principal absorption lines in the considered spectral region are $H_2O$, $CO_2$, $O_3$, $N_2O$, $CH_4$ and $HNO_3$. The altitude distributions of their mixing ratios were deduced previously by the groups in charge of the

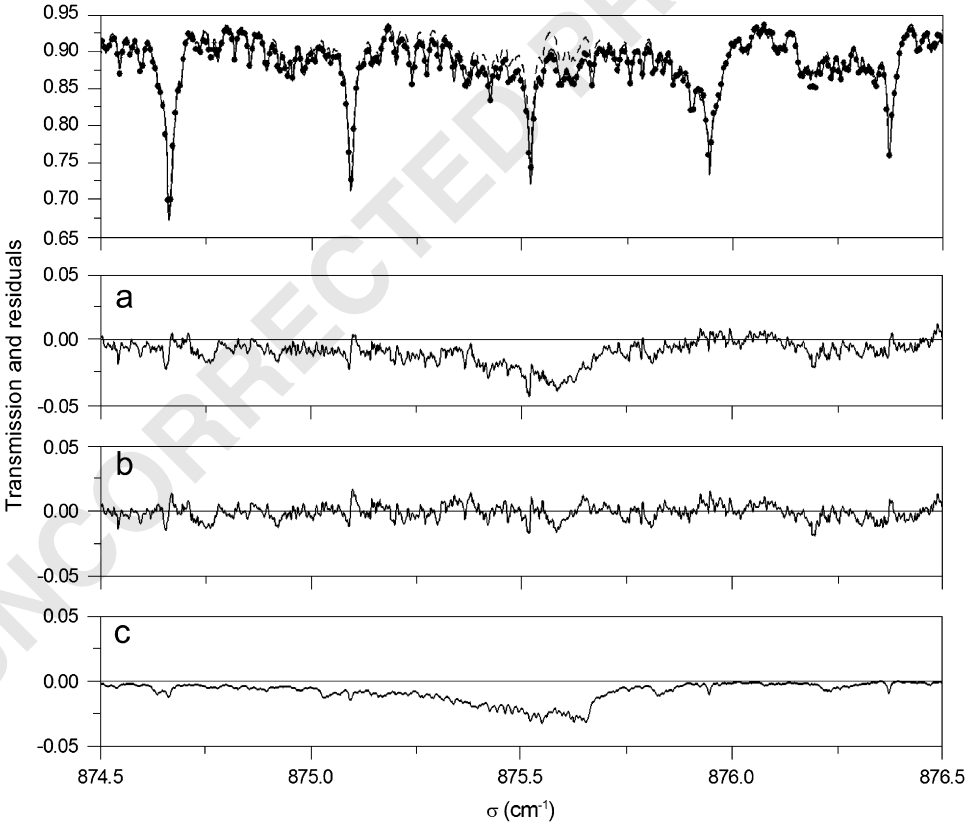


**Fig. 1.** Measured atmospheric transmission in the region of the $\nu_5+\nu_7-\nu_7$ for an elevation angle of 2.75° (●) and corresponding calculated values with (- - -) the old $HNO_3$ line list [17,19], and (—) the new improved one [18]. Plots in panels (a) and (b) are the corresponding differences between measured and calculated values. Panel (c) shows the difference between residuals reported in (a) and (b).



Please cite this article as: Tran H, et al. Validation of $HNO_3$ spectroscopic parameters using atmospheric absorption and emission measurements. JQSRT (2008), doi:10.1016/j.jqsrt.2008.09.012

instruments and, unless specified, are fixed in the present work. Similarly, the temperature and pressure profiles, the pointing geometry and the instrument response function, were determined independently and left unchanged in the calculations presented in the following section. Finally, aerosols and clouds are absent in all measurements used in this work and, in our calculations, only clear sky cases are thus considered.

## 3. Validation of the new database

### 3.1. Ground-based Fourier transform solar absorptions

Neglecting scattering and latitudinal and longitudinal inhomogeneities, the atmospheric transmission $\tau(\sigma)$ at wavenumber $\sigma$ is computed from

$$\tau(\sigma) = \int F_{\mathrm{Instr}}(\sigma - \sigma')\,\mathrm{d}\sigma' \times \exp\left[-\int_{z_{\mathrm{Inst}}}^{z_{\mathrm{Max}}} \sum_a \alpha_a[\sigma', x_a, T(z), p(z)]\frac{\mathrm{d}s}{\mathrm{d}z}(z)\,\mathrm{d}z\right], \quad (1)$$

where $F_{\mathrm{Instr}}$ is the area-normalized instrument function and the integration over altitude ($z$) is made along a curvilinear abscissa $s(z)$ following the line of sight. Note that the influence of the very narrow field of view is disregarded in Eq. (1). The sum is over all species "$a$" of significant contribution to absorption at wavenumber $\sigma'$. For a given absorbing molecule $a$, with mixing ratio $x_a$ under total pressure p at temperature $T$, the local value of the absorption coefficient $\alpha_a$ is given by

$$\alpha_a(\sigma, x_a, T, p) = x_a p \times \sigma\left[1 - \exp\left(-\frac{hc\sigma}{k_B T}\right)\right]\left\{\sum_{\ell_a}\frac{S_{\ell_a}(T)}{\sigma_{\ell_a}[1-\exp(-hc\sigma_{\ell_a}/kT]}\frac{1}{\gamma_a^D(\sigma_{\ell_a},T)}\sqrt{\frac{\ln 2}{\pi}}\right.$$
$$\left.\times \mathrm{Re}\left[W\left(\frac{\sigma - \sigma_{\ell a} - p\delta_{\ell_a}}{\gamma_a^D(\sigma_{\ell_a},T)/\sqrt{\ln 2}} + i\frac{p\gamma_{\ell_a}(T)}{\gamma_a^D(\sigma_{\ell_a},T)/\sqrt{\ln 2}}\right)\right]\right\}, \quad (2)$$

where the sum extends over the absorption lines $\ell_a$ of species "$a$". The second line of Eq. (2) corresponds to the normalized Voigt profile of the line $\ell_a$. The quantities ${\gamma_a}^D$, $\sigma_{\ell_a}$, $\gamma_{\ell_a}$, $\delta_{\ell_a}$, $S_{\ell_a}$ are the Doppler width ($\mathrm{cm}^{-1}$), the unperturbed line position ($\mathrm{cm}^{-1}$), the line broadening and shifting coefficients ($\mathrm{cm}^{-1}$/atm) and the integrated intensity ($\mathrm{cm}^{-2}$/atm). $W(x,y)$ is the complex probability function [25,26], and $Re[\ldots]$ denotes the real part which leads to the (assumed) Voigt profile.

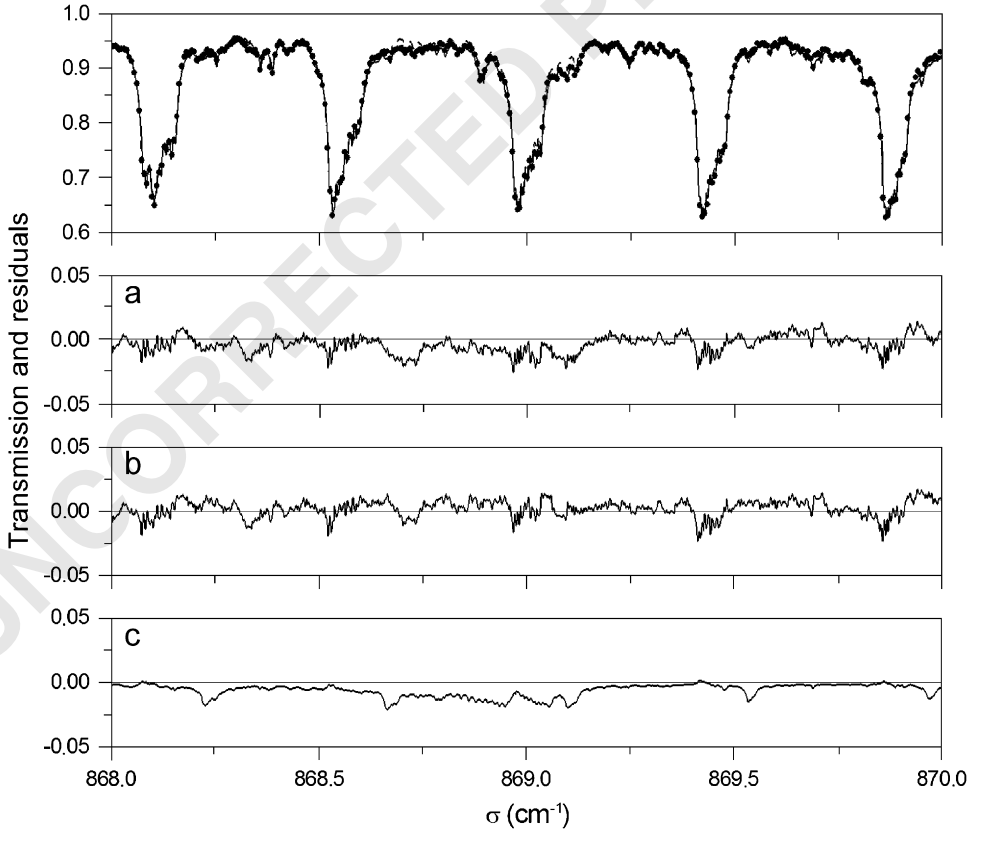


**Fig. 2.** Same as Fig. 1 but in the $\nu_5+\nu_6-\nu_6$ hot band region.



Please cite this article as: Tran H, et al. Validation of $HNO_3$ spectroscopic parameters using atmospheric absorption and emission measurements. JQSRT (2008), doi:10.1016/j.jqsrt.2008.09.012

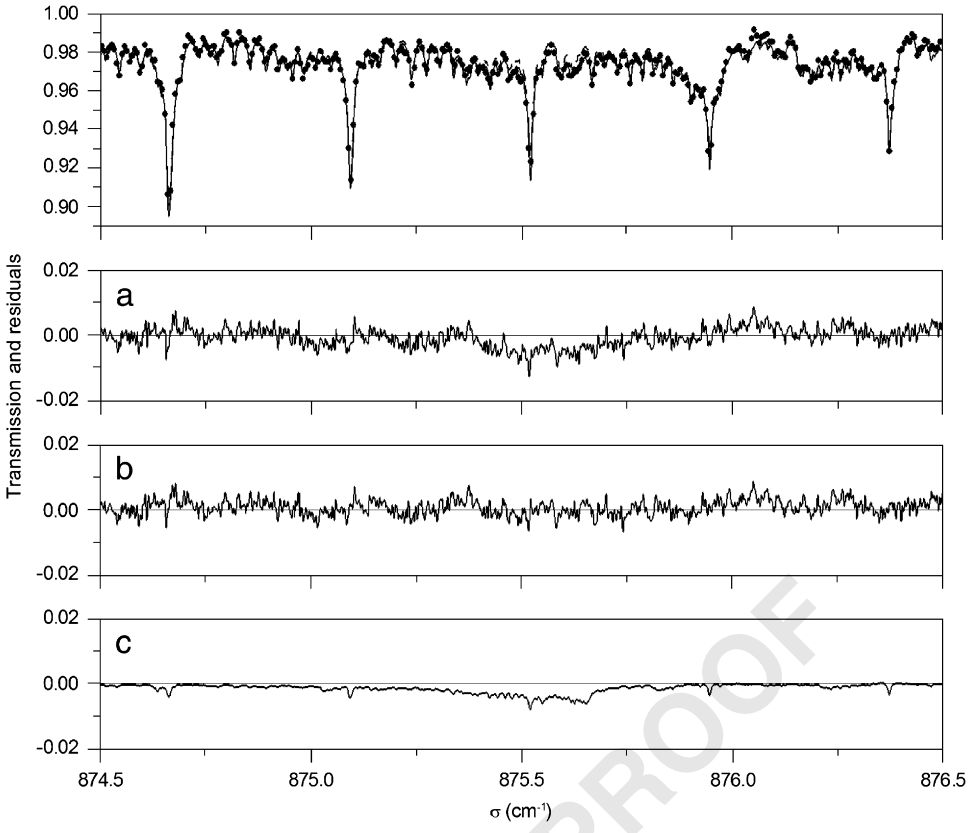


**Fig. 3.** Same as Fig. 1 but for an elevation angle of 14.50°.

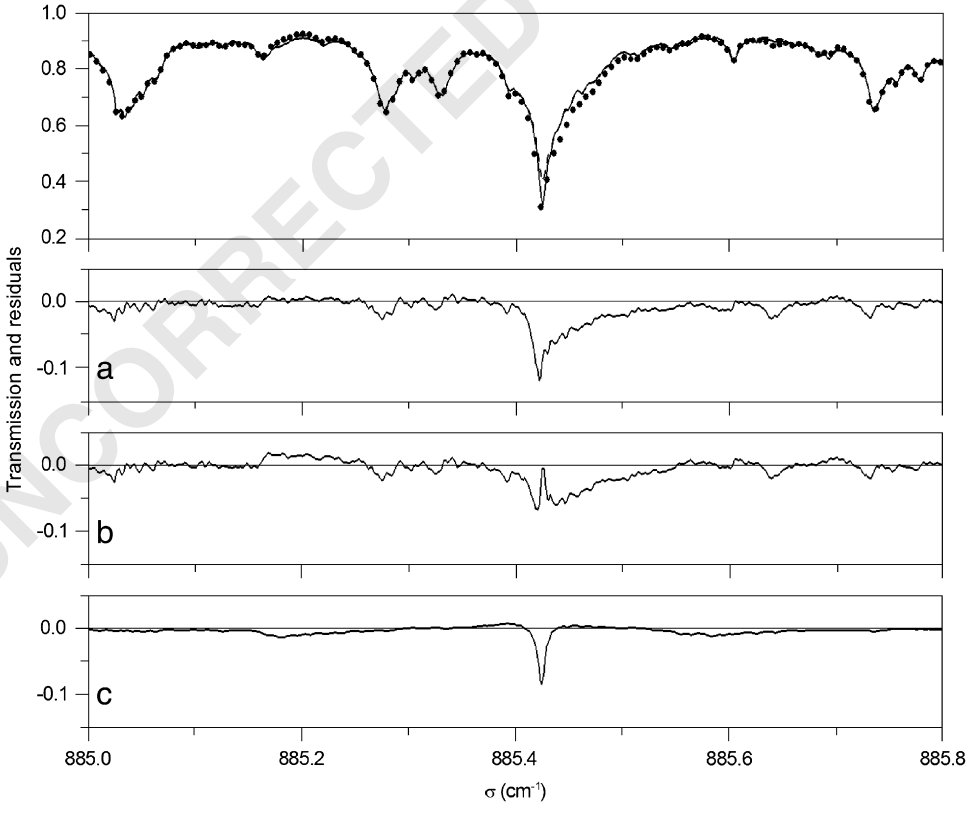


**Fig. 4.** Same as Fig. 1 but for the $v_5+v_9-v_9$ hot band region.

Note that the $HNO_3$ profile was originally deduced from these IMK spectra using the 2000 edition of the HITRAN database. Since the intensity of all lines of $HNO_3$ in the 820–950 $cm^{-1}$ region was decreased by about 11% from this edition to the version that we use here, the present calculations use $HNO_3$ amounts raised by 11%.

Comparisons between measured and calculated atmospheric transmissions for different spectral regions and two elevation angles are presented in Figs. 1–4. In all cases, calculations were performed using both the line parameter of the most recent HITRAN database and the modified line list proposed in Ref. [18]. In order to focus on the improvement brought by the new database, only the spectral regions where modifications were made are displayed. In Figs. 1 and 2, we show the results obtained in the intervals where the $\nu_5+\nu_7-\nu_7$ and $\nu_5+\nu_6-\nu_6$ hot bands were added. These regions are particularly important since they contain only $HNO_3$ transitions and are therefore often (partly) retained as micro-windows to retrieve the $HNO_3$ vmr [3,13,14]. As can be observed in Figs. 1 and 2, the new line list leads to significant improvements. This is confirmed, for another elevation angle (14.50°), in Fig. 3. Finally, a comparison between measurements and calculations using our new line list in the $\nu_5+\nu_9-\nu_9$ hot band is presented in Fig. 4. Recall that line-mixing effects within the Q branch of this band were detected and that a model was proposed in [18]. As shown in Fig. 4, line-mixing effects have a small but detectable influence on the atmospheric transmission, and the model of Ref. [18] leads to a better agreement with measurements.

### 3.2. SAO atmospheric emission spectra

The balloon-borne Fourier transform instrument of the SAO experiment measures atmospheric thermal emission in the 325–917 $cm^{-1}$ region. In this case, the quantity deduced from measurements is the radiance $I$, given by

$$I(\sigma) = \int_{FOV} d\Omega \int_{-\infty}^{+\infty} F_{Instr}(\sigma - \sigma') \times I^{Atm}(\sigma', d\Omega)\, d\sigma', \quad (3)$$

where the first integration is over the field of view (FOV) of the instrument and radiances are convolved by the normalized instrument function $F_{Instr}$. $I^{Atm}$ are spectral values of the intensity emitted by the atmosphere. Assuming local thermodynamic equilibrium, the latter are given by

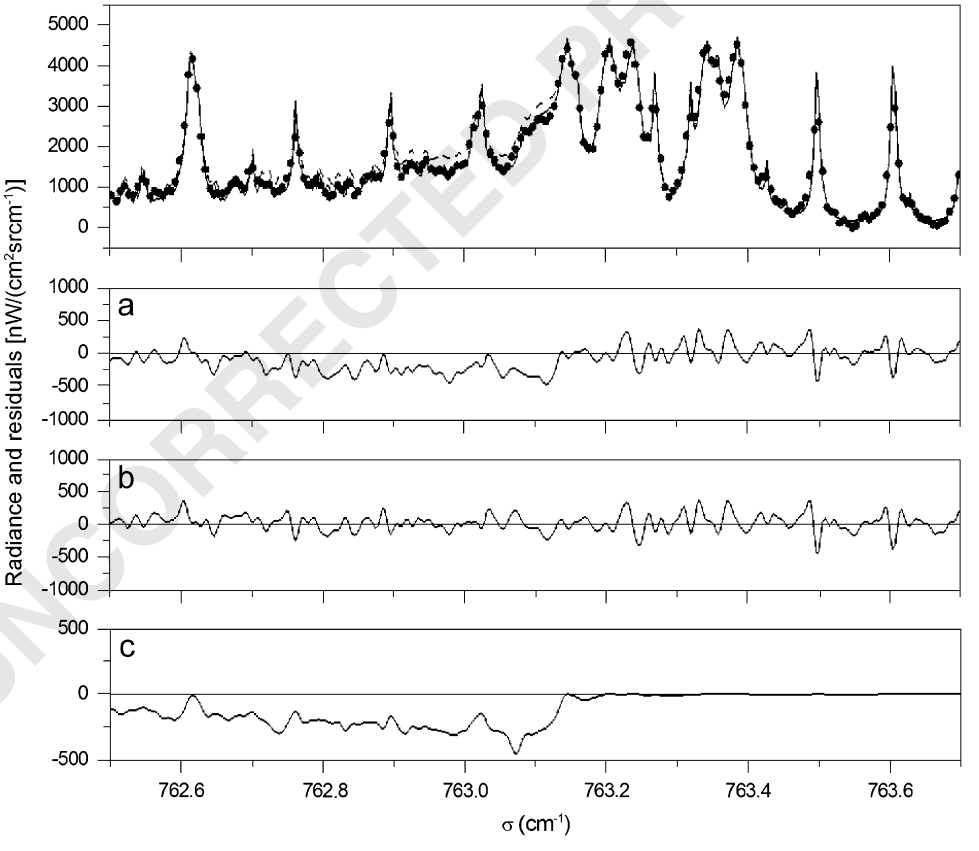


**Fig. 5.** SAO radiances collected from 36.7 km for a tangent height of 20.0 km. The upper part gives measurement and values calculated using (---) line parameters given in HITRAN and (—) line parameters of the improved list [18]. The curves in (a) and (b) are the corresponding measured–calculated deviations averaged over 0.01 $cm^{-1}$. Panel (c) shows the difference between residuals reported in (a) and (b).



Please cite this article as: Tran H, et al. Validation of $HNO_3$ spectroscopic parameters using atmospheric absorption and emission measurements. JQSRT (2008), doi:10.1016/j.jqsrt.2008.09.012

$$I^{\mathrm{Atm}}(\sigma,\mathrm{d}\Omega)=\int_{Z_{\mathrm{Obs}}}^{\infty}\left\{\sum_a \alpha_a[\sigma,x_a(z'),T(z'),p(z')]\times I_0[\sigma,T(z')]\right.$$
$$\left.\times\exp\left(-\sum_a\int_{Z_{\mathrm{Obs}}}^{Z'}\alpha_a[\sigma,x_a(z),T(z),p(z)]\frac{\mathrm{d}s}{\mathrm{d}z}(z,\mathrm{d}\Omega)\,\mathrm{d}z\right)\times\frac{\mathrm{d}s}{\mathrm{d}z}(z',\mathrm{d}\Omega)\,\mathrm{d}z'\right\}, \quad (4)$$

where $I_0$ is the black body radiance, and the absorption coefficient $\alpha_a$ of species "$a$" is calculated from Eq. (2), except in the case of $CO_2$ for which calculations are performed accounting for line-mixing using the model of Ref. [27]. Note that, for $H_2O$, a continuum is added to the local values of the absorption coefficient. These self- and air-broadened contributions, which are significant at long wavelengths, have been calculated using the CKD 2.4 data and software by Clough et al. [28]. This specific treatment for $CO_2$ and $H_2O$ is required here since higher frequencies are considered.

For $HNO_3$, the vmr profile was originally determined [29] from microwindows selected in the 22 μm region using $\nu_9$ band transitions with line intensities given in HITRAN [30], which were obtained through a scaling to the results of the $\nu_9$ band intensity measurements performed in Ref. [31]. Since this time, Sirota et al. [32] have suggested a significantly weaker value (~28%) for the $\nu_9$ band intensity but this result was not validated by further measurements. Hence we have left the original $HNO_3$ profile unchanged.

Figs. 5 and 6 present comparisons between measurements and calculations for the $\nu_8$ region and various tangent heights. The present calculations were performed using both the HITRAN line list and our new database [18] in which $\nu_8$ band line intensities were updated. As can be observed in these figures, a better agreement is obtained between the observed and calculated spectra when using the new parameters. On the other hand, when using HITRAN data, the calculations overestimate the emitted radiance in the 13.1 μm region lead. These results could indicate that there is a rather good consistency of the $\nu_8$ (in [18]) and $\nu_9$ [19,30] line intensities, while in HITRAN the ($\nu_8/\nu_9$) intensity ratio is about 20% too strong.

### 3.3. MIPAS measurements

The new $HNO_3$ database has also been validated by comparing MIPAS measurements with spectra generated using alternatively the old [17,19] and the new [18] line parameters. This procedure was successfully adopted to validate MIPAS PF3.2 $HNO_3$ line parameters as described in Ref. [17], where technical details can be found. The MIPAS measurements used

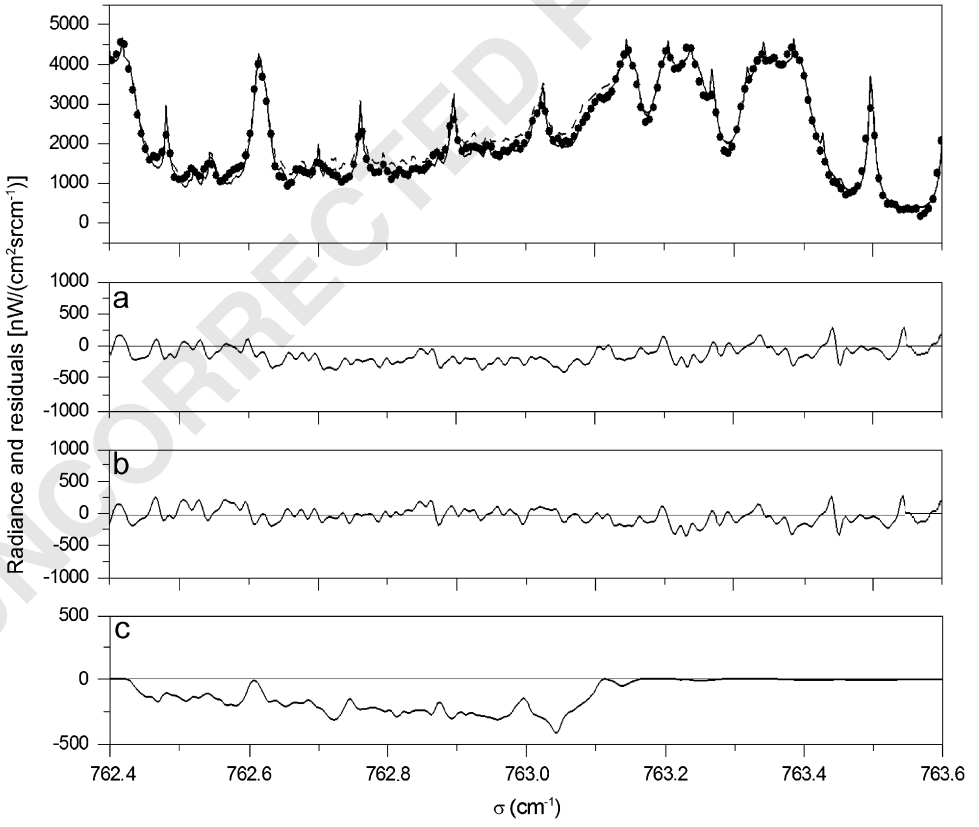


**Fig. 6.** Same as Fig. 5 bur for a tangent height of 15.9 km.



Please cite this article as: Tran H, et al. Validation of $HNO_3$ spectroscopic parameters using atmospheric absorption and emission measurements. JQSRT (2008), doi:10.1016/j.jqsrt.2008.09.012

in the present study are the same as those used for the previous validation, i.e, limb radiances selected among the observations acquired during orbits 2081 and 2082 (July 2002), for nominal tangent altitudes of 12 and 24 km. The corresponding simulations were calculated by using the two-dimensional forward model available at Bologna University. Three sets of synthetic spectra, in the 750–930 $cm^{-1}$ spectral range (sub-interval of MIPAS band A), were generated using the two $HNO_3$ spectroscopic datasets and different vertical distribution profiles. The first set (labeled S1) uses the old spectroscopic database and $HNO_3$ vmr profiles retrieved by the MIPAS off-line processor operated with the same spectroscopic information. For the second set (S2), the same $HNO_3$ vmr profiles were used but with the new spectroscopic database [18]. In the third set of simulations (S3), both the new line list and $HNO_3$ vmr profiles retrieved with these new parameters were used. In all three cases, the retrieval of the $HNO_3$ vertical distributions used the 876.375–879.375 $cm^{-1}$ and 885.100–888.100 $cm^{-1}$ spectral intervals. For each set of spectra, the differences between observed spectrum and the corresponding simulation were averaged and corrected using the residual and error correlation analysis technique. The results of this analysis, presented in Table 1, clearly show that the new database leads to improved results in term of both average and root mean square (RMS) residuals. Note that the differences between the vmr profiles retrieved by the new line list and the old spectroscopic database are of about 2‰. MIPAS measured spectra and differences with respect to calculated

**Table 1**
Characterization of the residuals obtained comparing MIPAS observed spectra with simulated spectra of type S1 and S3, for tangent height of 12 and 24 km

| Simulation type and database version | Tangent height of 12 km | | Tangent height of 24 km | |
|---|---|---|---|---|
| | Average difference | RMS | Average difference | RMS |
| S1—Old database | 2.27 | 24.30 | 1.30 | 18.56 |
| S3—New database | −0.93 | 20.50 | −0.22 | 16.09 |

The results are in nW/($cm^2$ sr $cm^{-1}$).



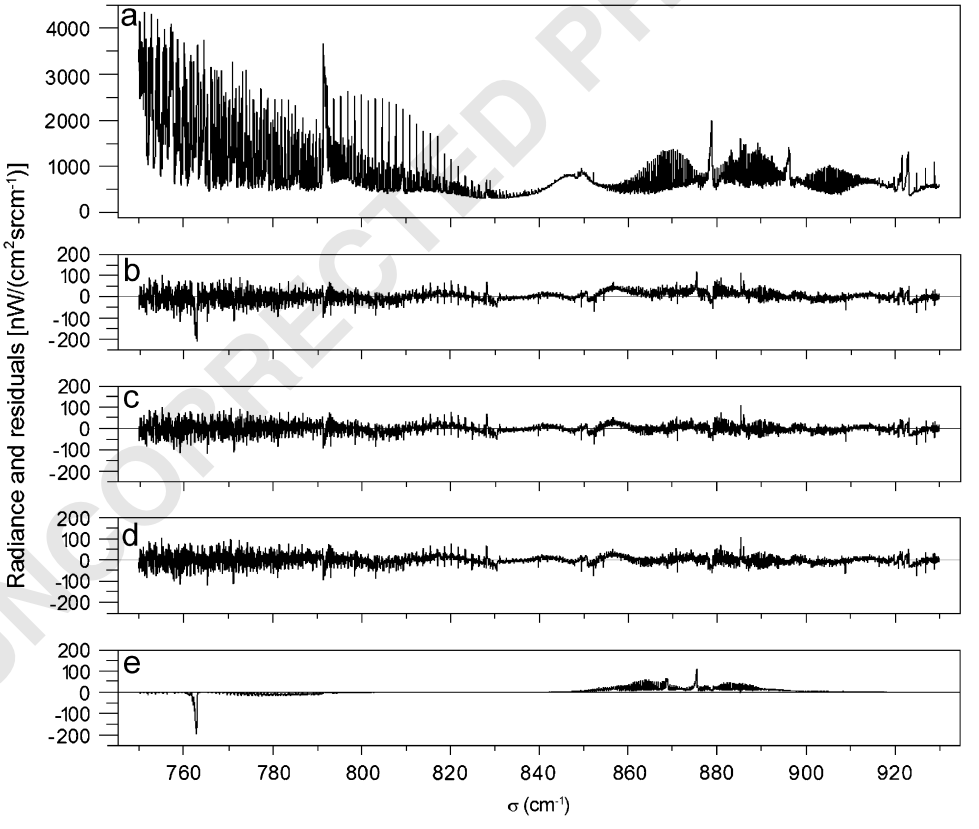


**Fig. 7.** (a): average of 55 MIPAS spectra acquired during orbits 2081 and 2082 for a sub-interval of band A, at tangent altitude of 12 km. Panels (b), (c) and (d) show the REC-corrected average residuals from simulations of type S1, S2 and S3, respectively (see text for details). Panel (e) shows the difference between residuals reported in (b) and (d).

Please cite this article as: Tran H, et al. Validation of $HNO_3$ spectroscopic parameters using atmospheric absorption and emission measurements. JQSRT (2008), doi:10.1016/j.jqsrt.2008.09.012

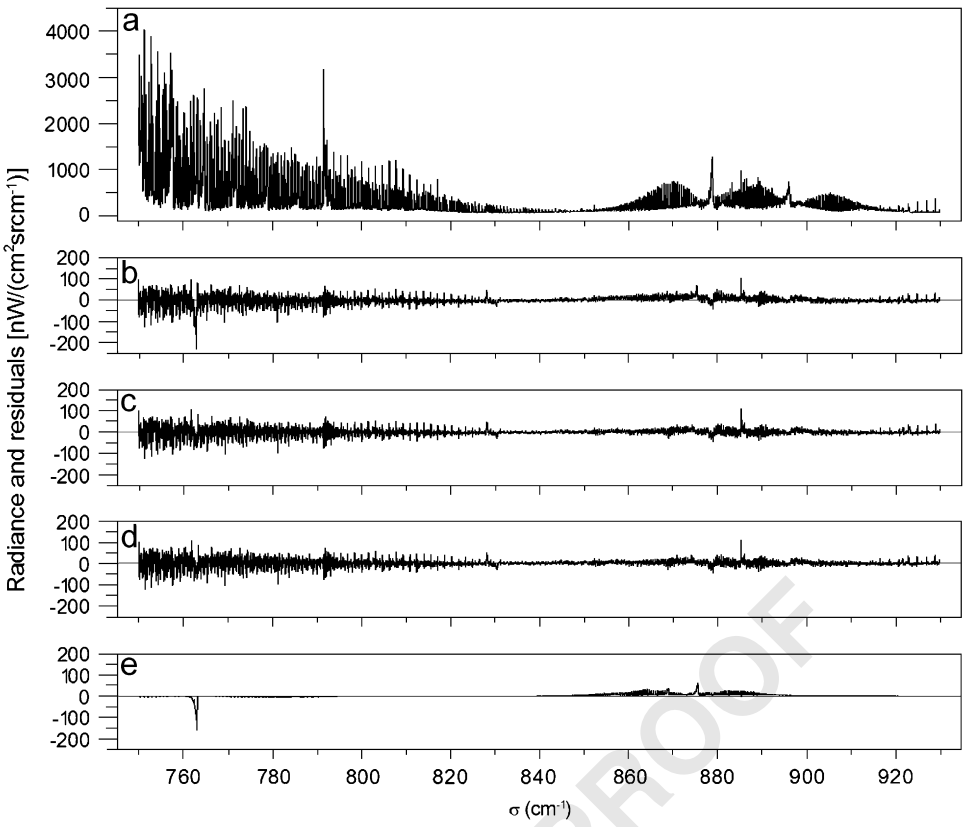


**Fig. 8.** Same as Fig. 7 but for a tangent height of 24 km.

results obtained from limb radiance simulations of type S1, S2 and S3 are reported in Figs. 7 and 8 for tangent heights of 12 and 24 km, respectively. These plots visually confirm the improvement achieved in both the 11 and 13 μm regions.

## 4. Conclusion

The results obtained in the present paper confirm the improvement achieved by the new line list [18]. Furthermore, the comparisons between calculations and MIPAS and SAO spectra are in favor of an overall consistency of the intensities for the 13.1 ($\nu_8$ band)–11 μm ($\nu_5/2\nu_9$) regions, and for the 22 ($\nu_9$)–13.1 μm regions, respectively. They confirm the conclusion of the previous paper stating that the band intensity ratio $\nu_8/(\nu_5/2\nu_9)$ is too strong in HITRAN [19] by about 20%. It is clear, however, that future laboratory studies are needed in order to get more accurate information, in particular for the hot bands whose line positions and intensities are still not fully satisfactory ($\nu_5+\nu_9-\nu_9$, [11]) and were generated in a rather crude way ($\nu_5+\nu_6-\nu_6$, $\nu_5+\nu_7-\nu_7$) in our previous paper. Finally, additional laboratory line intensities are still needed for the 22 μm bands ($\nu_9$ and corresponding hot bands) for which differing values as compared to those quoted in HITRAN were determined in Ref. [32].

## Acknowledgments

The authors thank Ken Jucks for communicating a set of SAO spectra. L. Gomez and A. Perrin thank the European Community for financial support within the "QUASAAR" (QUAntitative Spectroscopy for Atmospheric and Astrophysical Research) network project (Contract MRTN-CT-2004-512202). They also gratefully acknowledge a financial support from the French research program "Les Enveloppes Fluides et l'Environnnement, Chimie Atmosphérique" (LEFE-CHAT) from the "Institut National des Sciences de l'Univers" (INSU).

## Appendix A. Supporting Information

Supplementary data associated with this article can be found in the online version at doi:10.1016/j.jqsrt.2008.09.012.

## References

[1] Molina LT, Wang FC-Y. Antarctic stratospheric chemistry of chlorine nitrate, hydrogen chloride, and ice: release of active chlorine. Science 1987;238(4831):1253–7.
[2] Rinsland CP, Zander R, Demoulin P. Ground-based infrared measurements of $HNO_3$ total column abundances: long term trend and variability. J Geophys Res 1991;96(D5):9379–89.
[3] Hase F, Hannigan JW, Coffey MT, Goldman A, Höpfner M, Jones NB, et al. Intercomparison of retrieval codes used for the analysis of high-resolution, ground-based FTIR measurements. JQSRT 2004;87:25–52.
[4] Meier A, Paton-Walsh C, Bell W, Blumenstock T, Hase F, Goldman A, et al. Evidence of reduced measurement uncertainties from an FTIR instrument intercomparison at Kiruna, Sweden. JQSRT 2005;96:75–84.
[5] Goldman A, Murcray FJ, Blatherwick RD, Kosters JJ, Murcray FH, Murcray DG. New spectral features of stratospheric trace gases identified from high resolution infrared balloon borne and laboratory spectra. J Geophys Res 1989;94(D12):14945–55.
[6] Murcray FJ, Starkey JR, Willians WJ, Matthews WA, Schmidt U, Aimedieu P, et al. $HNO_3$ profiles obtained during the EASOE campaign. Geophys Res Lett 1994;21(13):1223–6.
[7] Camy-Peyret C, Payan S, Jeseck P, Té Y, Acad CR. Mesures spectroscopiques de constituants et de polluants atmosphériques par techniques in situ et à distance, au sol ou embarquées. Sci Paris Ser 2001;IV 2:905–22.
[8] Russell JM, Farmer CB, Rinsland CP, Zander R, Froidevaux L, Toon GC, et al. Measurements of odd nitrogen compounds in the stratosphere by the ATMOS experiment on Spacelab3. J Geophys Res 1988;93(D2):1718–36.
[9] Gunson MR, et al. The atmospheric trace molecule spectroscopy (ATMOS) experiment: deployment on the ATLAS space shuttle missions. Geophys Res Lett 1996;23(17):2333–6.
[10] Perrin A, Flaud JM, Camy-Peyret C, Goldman A, Rinsland P, Gunson MR. Identification of the $HNO_3$ $3\nu_9-\nu_9$ band Q branch in stratospheric solar occultation spectra. JQSRT 1994;52:319–22.
[11] Flaud JM, Perrin A, Orphal J, Kou Q, Flaud PM, Dutkiewicz Z, et al. New analysis of the $\nu_5+\nu_9-\nu_9$ hot band of $HNO_3$. JQSRT 2003;77:355–64.
[12] Koike, et al. A comparison of arctic $HNO_3$ profiles measured by the limb atmospheric spectrometer and balloon-borne sensors. J Geophys Res 2000;105(D5):6761–71.
[13] Griesfeller A, Griesfeller J, Hase F, Kramer I, Loes P, Mikuteit S, et al. Comparison of ILAS-II and ground-based FTIR measurements of $O_3$, $HNO_3$, $N_2O$, and $CH_4$ over Kiruna, Sweden. J Geophys Res 2006;111:D11S07.
[14] Von Clarmann T, Fischer H, Friedl-Vallon F, Linden A, Oelhaf H, Piesch C, et al. Retrieval of stratospheric $O_3$, $HNO_3$ and $ClONO_2$ profiles from 1992 MIPAS-B Limb emission spectra: method, results and error analysis. J Geophys Res 1993;98(D11):20495–506.
[15] Blom CE, Fischer H, Glatthor N, Gulde T, Höpfner M, Piesch C. Spatial and temporal variability of $ClONO_2$, $HNO_3$ and $O_3$ in the Arctic winter of 1992/1993 as obtained by airborne infrared emission spectroscopy. J Geophys Res 1995;100(D5):9101–14.
[16] Ridolfi M, Carli B, Carlotti M, von Clarmann T, Dinelli BM, Dudhia A, et al. Optimized forward model and retrieval scheme for MIPAS near-real-time data processing. Appl Opt 2000;39(8):1323–40.
[17] Flaud JM, Brizzi G, Carlotti M, Perrin A, Ridolfi M. MIPAS database: validation of $HNO_3$ line parameters using MIPAS satellite measurements. Atmos Chem Phys 2006;6:5037–48.
Q1 [18] Gomez L, Tran H, Perrin A, Gamache RR, Laraia A, Orphal J, et al. Some improvements of the $HNO_3$ spectroscopic parameters in the spectral region from 600 to 950 $cm^{-1}$. JQSRT 2008, in press.
[19] Rothman LS, Jacquemart D, Barbe A, Benner DC, Birk M, Brown LR, et al. The HITRAN 2004 molecular spectroscopic database. JQSRT 2005;96:139–204.
[20] Laraia A, Gamache RR, Hartmann JM, Perrin A, Gomez L. Calculations of $N_2$ pressure-broadened half widths for $HNO_3$. JQSRT 2008, in preparation.
[21] Perrin A, Puzzarini C, Colmon JM, Verdes C, Wlodarczak G, Cazzoli G, et al. Molecular line parameters for the "MASTER" (millimeter wave acquisitions for stratosphere/troposphere exchange research) database. J Atmos Chem 2005;51:161–205.
[22] Kopp G, Berg H, Blumenstock T, Fischer H, Hase F, Hochschild G, et al. Evolution of ozone and ozone related species over Kiruna during the THESEO 2000-SOLVE campaign retrieved from ground-based millimeter wave and infrared observations. J Geophys Res 2003;108:8308–14.
[23] Johnson DG, Jucks KW, Traub WA, Chance KV. Smithsonian stratospheric far-infrared spectrometer and data reduction system. J Geophys Res 1995;100:3091–106.
[24] Endemann M. MIPAS instrument concept and performance. In: proceedings of the ESAM'99, ESTEC-ESA, WPP-161, 1, 29-43, ISSN 1022-6656; 1999.
[25] Humlicek J. An efficient method for evaluation of the complex probability function: the Voigt function and its derivatives. JQSRT 1979;21:309–13.
[26] Wells RJ. Rapid approximation to the Voigt/Faddeeva function and its derivatives. JQSRT 1999;62:29–48.
[27] Niro F, Boulet C, Hartmann JM. Spectra calculations in central and wing regions of $CO_2$ IR bands between 10 and 20 μm. I: model and laboratory measurements. JQSRT 2004;88:483–98.
[28] The up to date version of the CKD2 continue and associated software by Clough et al. are included in the LBLRTM radiative transfer code and can be downloaded from the web site of Atmospheric and Environmental Research (AER), Inc. at the address 〈http://www.rtweb.aer.com/lblrtm_code.html〉. Some information is also given in: Clough SA, Iacono MJ, Moncet JL, editors. Line by line calculations of atmospheric fluxes and cooling rates: applications to water vapour. J Geophys Res 1992;97:15761–85.
[29] Jucks KW, Johnson DG, Chance KV, Traub WA. Nitric acid in the middle stratosphere as a function of altitude and aerosol loading. J Geophys Res 1999;104(D21):26715–23.
[30] Goldman A, Rinsland CP, Perrin A, Flaud JM. $HNO_3$ line parameters: 1996 HITRAN update and new results. JQSRT 1998;60:851–61.
[31] Goldman A, Bonomo FS, Williams WJ, Mucray DG. Statistical band model analysis and integrated intensity for the 21.8 μm bands of $HNO_3$ vapor. J Opt Soc Amer 1975;65:10–2.
[32] Sirota JM, Weber M, Reuter DC, Perrin A. $HNO_3$: absolute line intensities for the $\nu_9$ fundamental. J Mol Spectr 1997;184:140–4.



Please cite this article as: Tran H, et al. Validation of $HNO_3$ spectroscopic parameters using atmospheric absorption and emission measurements. JQSRT (2008), doi:10.1016/j.jqsrt.2008.09.012